

CDR-restricted engineering of native human scFvs creates highly stable and soluble bifunctional antibodies for subcutaneous delivery

Brian J Fennell^{1,†}, Barry McDonnell^{1,†}, Amy Sze Pui Tam², Lijun Chang³, John Steven³, Ian D Broadbent³, Huilan Gao², Elizabeth Kieras⁴, Jennifer Alley⁴, Deborah Luxenberg⁴, Jason Edmonds⁴, Lori J Fitz⁴, Wenyan Miao⁴, Matthew J Whitters⁴, Quintus G Medley⁴, Yongjing J Guo², Alfredo Darmanin-Sheehan¹, Bénédicte Autin¹, Deirdre Ní Shúilleabháin¹, Emma Cummins¹, Amy King², Mark RH Krebs², Christopher Grace⁵, Timothy P Hickling⁵, Angela Boisvert², Xiaotian Zhong², Matthew McKenna², Christopher Francis², Stephane Olland², Laird Bloom², Janet Paulsen², Will Somers², Allan Jensen², Laura Lin², William JJ Finlay¹, and Orla Cunningham^{1,*}

¹Pfizer; Global Biotherapeutics Technologies; Dublin, Ireland; ²Pfizer; Global Biotherapeutics Technologies; Cambridge, MA USA; ³Pfizer; Global Biotherapeutics Technologies, Foresterhill; Aberdeen, UK; ⁴Pfizer; Immunoscience; Cambridge, MA USA; ⁵Pfizer; Pharmacokinetics, Dynamics, and Metabolism; Sandwich, UK

[†]These authors contributed equally to this work.

Keywords: affinity optimization, phage display, thermal stability, high concentration formulation, bispecific scFv-Fc-scFv

Abbreviations: CDR, complementarity determining region; ScFv, single-chain Fv antibody fragment; V_H, variable region of the heavy chain; V_L, variable region of the light chain; IgG, immunoglobulin G; HRP, horseradish peroxidase; PBS, phosphate-buffered saline; HBS-EP, HEPES buffered saline-phosphate; BSA, bovine serum albumin; RU, response units; Fw, framework; HMW, high molecular weight; IPTG, isopropyl-β-DI-thiogalactopyranoside; HTRF, homogenous time-resolved fluorescence transfer; Tb IP-One, terbium inositol phosphate-one; cP, centipoise; SEC, size-exclusion chromatography; QC, quality control; SOE-PCR, splice-overlap-extension polymerase chain reaction; IV, intravenous; PK, pharmacokinetic

While myriad molecular formats for bispecific antibodies have been examined to date, the simplest structures are often based on the scFv. Issues with stability and manufacturability in scFv-based bispecific molecules, however, have been a significant hindrance to their development, particularly for high-concentration, stable formulations that allow subcutaneous delivery. Our aim was to generate a tetravalent bispecific molecule targeting two inflammatory mediators for synergistic immune modulation. We focused on an scFv-Fc-scFv format, with a flexible (A₄T)₃ linker coupling an additional scFv to the C-terminus of an scFv-Fc. While one of the lead scFvs isolated directly from a naïve library was well-behaved and sufficiently potent, the parental anti-CXCL13 scFv 3B4 required optimization for affinity, stability, and cynomolgus ortholog cross-reactivity. To achieve this, we eschewed framework-based stabilizing mutations in favor of complementarity-determining region (CDR) mutagenesis and re-selection for simultaneous improvements in both affinity and thermal stability. Phage-displayed 3B4 CDR-mutant libraries were used in an aggressive “hammer-hug” selection strategy that incorporated thermal challenge, functional, and biophysical screening. This approach identified leads with improved stability and >18-fold, and 4 100-fold higher affinity for both human and cynomolgus CXCL13, respectively. Improvements were exclusively mediated through only 4 mutations in V_L-CDR3. Lead scFvs were reformatted into scFv-Fc-scFvs and their biophysical properties ranked. Our final candidate could be formulated in a standard biopharmaceutical platform buffer at 100 mg/ml with <2% high molecular weight species present after 7 weeks at 4 °C and viscosity <15 cP. This workflow has facilitated the identification of a truly manufacturable scFv-based bispecific therapeutic suitable for subcutaneous administration.

Introduction

A combination of advances in antibody engineering technologies and our understanding of the multi-pathway signaling in the pathogenesis of complex diseases have highlighted the potential for multi-targeting biotherapeutics. Bispecific antibodies have

many potential modes of action, including engagement of multiple epitopes on a single target, neutralization of two targets in a disease pathway or simply an increase in stoichiometric ratio of therapeutic agent to antigen.¹ The net result in each case should be improved efficacy over a traditional monoclonal IgG therapy. To be a viable drug, a bispecific molecule must demonstrate

*Correspondence to: Orla Cunningham; Email: orla.cunningham@pfizer.com
Submitted: 07/24/13; Revised: 08/16/13; Accepted: 08/17/13
<http://dx.doi.org/10.4161/mabs.26201>

potency and long in vivo half-life, and be well-expressed and amenable to scale-up in a manufacturing environment, with good stability and low aggregation characteristics.^{2,3} The modular nature of antibody domain structures has been manipulated and engineered to generate a wide variety of bispecific formats, although few have managed to successfully recapitulate the favorable properties that can make monoclonal IgGs such good drug candidates.¹

An increasing number of bispecific antibody formats, however, are entering clinical studies and one has been approved. Blinatumomab⁴ is a bispecific, single-chain antibody consisting of an anti-CD19 scFv linked in tandem with an anti-CD3 scFv for T-cell engagement that has recently demonstrated efficacy in B-lineage acute lymphoblastic leukemia patients in a Phase 2 trial.⁵ Catumaxomab is a monoclonal, bispecific, trifunctional antibody that was approved in Europe for the intraperitoneal treatment of malignant ascites in 2009.^{6–8} The product's bispecificity is achieved via heterodimeric pairing of mouse IgG2a and rat IgG2b, with one antigen-binding site specific for CD3 and the second for the tumor antigen EpCAM. The Fc effector functionality of the antibody also contributes to the resulting complex immune reaction at the tumor site, leading to the effective elimination of tumor cells. Importantly, in both these cases, microgram quantities of the drug are administered by slow intravenous infusion or intraperitoneal injection. This route of administration, combined with very low dosing concentrations, ameliorates the need for the high concentration formulation that is a common hurdle for antibody drug candidates for inflammatory diseases, where efficient and convenient subcutaneous dosing is highly desirable.

The primary advantage of the scFv building block used in blinatumomab is the low complexity associated with a single polypeptide chain. In general, however, development of scFv-based therapeutics has been limited by scale-up issues often associated with their low stability and high propensity to aggregate, particularly at high concentrations. The antibody variable domains used in bispecific molecules are often reformatted from pre-existing, humanized, monoclonal antibodies, and may not maintain the biophysical attributes of the parental molecule in their new context. Indeed, it has been shown in some cases that V_H - V_L pairing stability can be dramatically reduced in the absence of the constant domains of the parental Fab.⁹ Stability optimization of v-domain pairing can be achieved through methods such as optimization of domain orientation and linkers;^{10,11} introduction of inter-chain disulphide bonds^{12,13} or knowledge-based engineering of frameworks/ V_H - V_L interface residues.^{2,14} Recent reports have also highlighted the importance of pre-selection of stable scFv building blocks for the effective development of stable IgG-scFv and scFv-Fc-scFv bispecific molecules.^{3,11} Despite these findings, to our knowledge there have been no reports of such molecules being stable and sufficiently soluble for high-concentration formulation.

In this study, we endeavored to engineer a tetravalent scFv-Fc-scFv molecule, targeting two immunomodulatory targets, the soluble chemokine CXCL13, and a cell-surface inflammatory antigen. A screening workflow was implemented to identify a

final lead molecule with exemplary stability and solubility at high concentration that would permit subcutaneous delivery formulations and facilitate low-frequency dosing. This required optimization of the anti-CXCL13 scFv building block for both affinity and stability, and was achieved exclusively through mutation of the V_L -CDR3 without any additional non-natural framework manipulation. The resulting molecule was expressed and purified using standard scalable monoclonal antibody platforms and was shown to be amenable to high concentration formulation at 100 mg/ml in a standard pharmaceutical buffer with no adverse aggregation or viscosity. We demonstrate for the first time that, when native, human scFvs are aggressively optimized to function in that format, the high concentration formulation required for subcutaneous delivery of scFv-based bispecifics and low-frequency dosing is an achievable goal.

Results

Investigating the C-terminal CH3-scFv linker in POC scFv-Fc-scFvs. The scFv-Fc-scFv format is shown in **Figure 1A**, indicating the positioning of three linkers of interest (A4T, G4S, and CL) between the CH3 domain and the C-terminal scFv. Prototype scFv-Fc-scFvs were produced by transient transfection of 293 cells. Protein A purification followed by size-exclusion chromatography (SEC) typically resulted in yields of 20–30 mg/L for all three constructs, which is consistent with our experience of other human Fc-based proteins expressed in the same system (data not shown). The three scFv-Fc-scFv constructs all used the same pairs of scFv binding domains, which were isolated during quality control (QC) screening of in-house phage display libraries derived from the naïve human B-cell repertoire. The N-terminal binding domain was isolated against human tumor necrosis factor (TNF) and the C-terminal binding domain was specific for fluoresceinated bovine serum albumin (FITC-BSA), a routine QC antigen for phage display libraries.^{15–17} A dual-binding ELISA was developed whereby one antigen was immobilized and incubated with scFv-Fc-scFv, followed by a biotinylated form of the second antigen. This was subsequently detected with streptavidin-HRP. No significant difference in binding signal was observed with either FITC-BSA or TNF immobilization, indicating that all scFv-Fc-scFv formats support concomitant dual antigen binding. Representative data for scFv-Fc-scFv binding to immobilized FITC-BSA with streptavidin detection of bound TNF-biotin is shown in **Figure 1B**. The potential for C-terminal linker modulation of scFv-Fc-scFv stability was also monitored by differential scanning calorimetry (DSC). All three constructs showed overlapping thermograms with no significant difference between individual domain T_m values (**Fig. 1C**).

An intravenous pharmacokinetic (PK) study in rats was then performed to determine if the bispecific scFv-Fc-scFvs recapitulated the favorable half-life profile associated with monoclonal antibodies, and to evaluate the role of the C-terminal linkers on in vivo clearance rates. Each construct was administered at 1 mg/kg into groups of three rats each, and serum ELISAs against TNF and FITC-BSA were performed at regular time points. The

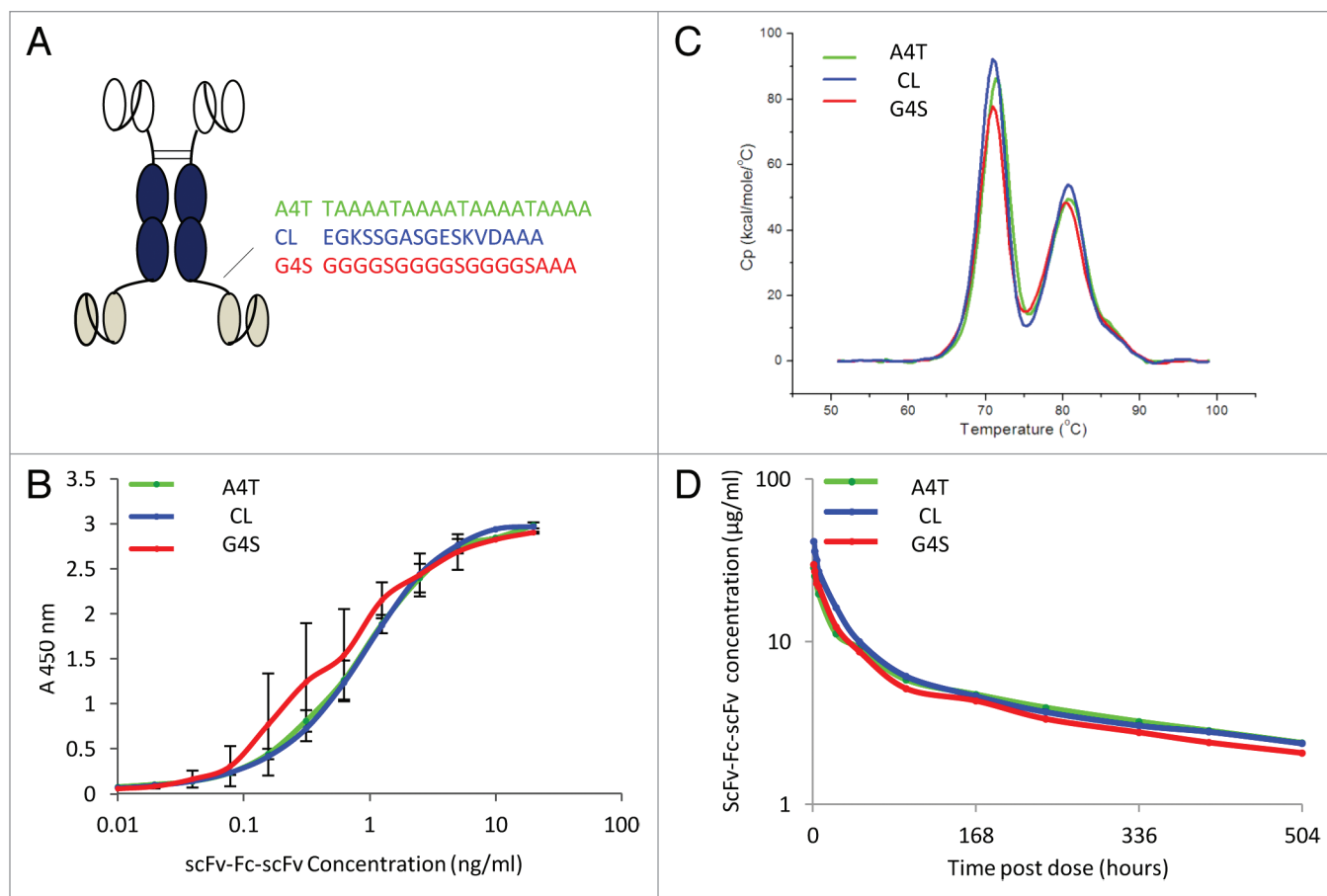


Figure 1. In vitro and in vivo characterization of C-terminal linkers. **(A)** Schematic of scFv-Fc-scFv format with associated C-terminal linker sequences. **(B)** Dual-specificity binding ELISA showing scFv-Fc-scFvs binding concomitantly to immobilized FITC-BSA and biotinylated-TNF via detection of streptavidin-HRP. **(C)** Comparative DSC analysis of C-terminal scFv-Fc-scFv variants measured at 0.3 mg/ml in PBS, pH 7.2. **(D)** Comparative rat PK study following scFv-Fc-scFv intravenous injection at 1 mg/kg.

serum ELISAs showed no significant differences between the three constructs whether the binding to TNF or FITC-BSA was used to monitor circulating ScFv-Fc-scFv levels. The elimination phase showed a linear decay over time for the three constructs, with no evidence of the rapid nonlinear decay that might be indicative of an immediate anti-drug antibody (ADA) response or a target-mediated clearance effect (Fig. 1D). The choice of C-terminal linker did not significantly affect any of the PK values measured, with all three constructs having mean elimination half-lives of over 300 h, while mean clearance rates were also very similar (0.28–0.29 ml/h/kg). These results compare favorably with previously documented human IgG1 PK in rats, with an elimination half-life of 128 h and a clearance of 0.80 ml/h/kg.¹⁸ PK measurements are summarized in Table S1. Because none of the 3 linkers tested were found to significantly affect in vitro or in vivo function of the scFv-Fc-scFv construct, we chose the A4T linker for all subsequent constructs.

Characterization of anti-CXCL13 domain 3B4. ScFv domains against CXCL13 (3B4, V_H1–69/V_L2–14) and a cell surface target herein named Immunomodulatory Target 1 (IT1; V_H3–30/V_L1–44) were isolated from in-house phage display libraries using standard methods (data not shown). Despite

achieving potent neutralization of the hCXCL13-CXCR5 interaction in an IP-One assay (data not shown), the anti-CXCL13 domain 3B4 had sub-optimal affinities for both human and cynomolgus CXCL13 when formatted as scFv-Fc. Biacore analysis revealed an apparent K_D value of 0.37 nM for human CXCL13. It should be noted that the phrase “apparent K_D” is used here to indicate where K_a approaches 10⁷ M⁻¹ s⁻¹, which is the point at which Biacore technology ceases to be fully accurate. While this is a reasonable affinity for a primary isolate from a human scFv library, the interaction showed a relatively fast off-rate (0.0121 s⁻¹). As the measured K_D was also 100-fold lower for cynomolgus CXCL13, these observations provided a strong rationale for off-rate optimization of 3B4 to normalize its affinity for the human and cynomolgus orthologs.

Many of the viability issues associated with scFv-based bispecific antibodies have been attributed to poor stability, and, therefore, we wanted to incorporate stability screening into early analyses of our reformatted scFv-Fc-scFvs. An initial panel of test molecules were constructed using a combination of two different IT1 scFvs and the CXCL13 scFv 3B4. The thermal stabilities of each protein were then assessed. ScFv-Fc-scFvs constructed exclusively from IT1 scFvs had good thermal stability with T_m values

all > 66 °C (Fig. 2); however, constructs containing 3B4 had significantly lower T_m values in the range of 57 °C, providing an early indication that 3B4 also suffered from sub-optimal stability properties. An integrated optimization approach incorporating simultaneous selection and screening for affinity, cross-species reactivity, and thermal stability was therefore undertaken to identify anti-CXCL13 scFvs suitable for incorporation into therapeutic scFv-Fc-scFv molecules.

CDR-based engineering of anti-CXCL13 domain 3B4. Figure 3 illustrates the workflow that was used in the construction and selection of 3B4 optimization libraries. V_H -CDR3 and V_L -CDR3 mutagenesis was achieved using a classical degenerate oligo randomization approach.¹⁹ In addition, a spiking mutagenesis library was built for each CDR using mutagenic primers that aimed to incorporate approximately 50% wild-type and 50% any other amino acid at each position across each CDR3.²⁰ The 8 resulting libraries were constructed and analyzed by sequencing 96 clones from each to ensure successful incorporation of amino acids to form a functional library in accordance with the design. Each library was rescued independently and mixed into a single master pool for selection.

The phage pool was subsequently subjected to what we term a “Hammer-Hug” selection. Under these conditions, a highly stringent first round was performed with low target antigen concentration (biotinylated) and aggressive off-rate competition overnight (with non-biotinylated target), followed by a rescue round with higher antigen concentration in the absence of off-rate selection. Given the positively-charged nature of the CXCL13 antigen, we had some concerns that selections would be dominated by an excess of charge-based interactions, e.g., salt bridges, which may cause broader specificity issues and lead to an unusually high pI for the final antibody. For this reason, selections were performed in the presence of a large excess of positively-charged histones in the blocking buffer. All outputs were expressed as scFv in crude periplasmic extracts and screened in a competition HTRF assay that assessed performance against the parental 3B4 scFv. It was immediately clear that this approach resulted in a strongly enriched population of output clones that out-competed the parental molecule, which was highly suggestive of successful affinity optimization (Fig. 4A). Sequence analysis of the output clones indicated that mutation in V_L -CDR3 was exclusively favored in the best-performing clones, and there was no evidence of any enrichment of negative charge in either CDR3 loop.

We also performed an alternative branch of selection with the aim of driving toward more stable scFv building blocks for our bi-functional molecule. Outputs from Round 1 were pooled and subjected to a thermal challenge at 60 °C or 70 °C before

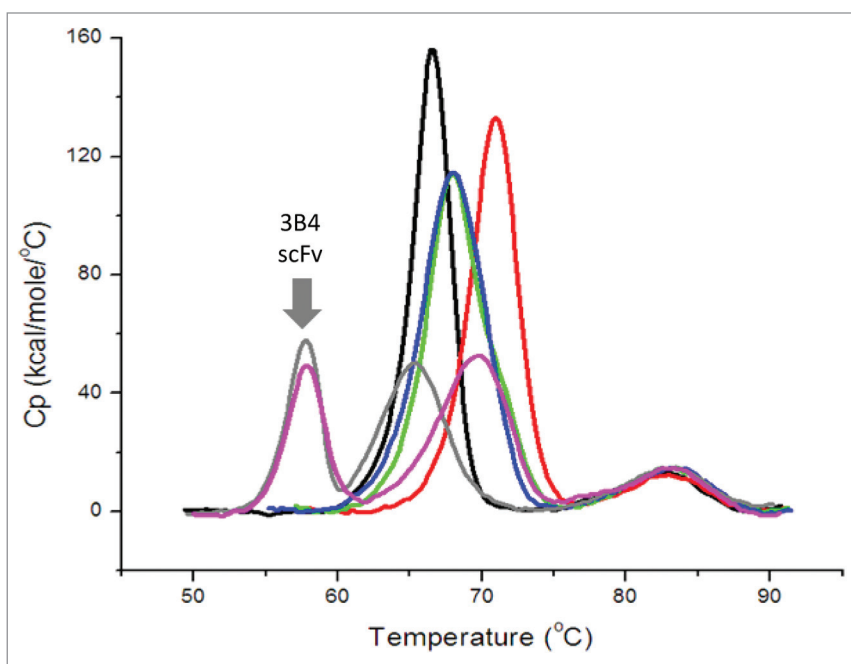


Figure 2. Thermal stability characteristics of scFv-Fc-scFv proteins containing combinations of two anti-IT1 lead scFvs (red, green, blue and black traces) or these anti-IT1 scFvs together with anti-CXCL13 3B4 (pink and gray traces), as measured in DSC. In both scFv-Fc molecules containing the 3B4 scFv, a low T_m was observed, suggesting that 3B4 was thermally unstable.

rescue with high antigen concentration. Figure 4B summarizes the HTRF screening data for these selection outputs. A significant shift in population was observed post-selection at both temperatures, with sequence analysis again illustrating dominance of V_L -CDR3 mutations and V_H -CDR3 showing little tolerance for functional mutation.

All of the top-performing scFvs in both assays (boxed) with unique sequences were taken forward for further analysis. These clones were expressed and purified at small scale in *E. coli* using nickel-based 96-well purification methods. Purified scFvs were titrated in a competition HTRF and ranked relative to the parental 3B4 scFv (Fig. 4C). The top 48 scFv clones from this assay were reformatted to scFv-Fc fusion proteins (scFv at N-terminus) and compared across all subsequent analyses. In each case, data are reported for a sub-population of these 48 scFv-Fc fusion proteins, representing the top performing clones from round 2 selection outputs with (clones E10, H8, and C7) and without (clones A1, H6, C4) thermal challenge. The reformatted scFv-Fc fusion proteins were then assayed in an IP-one CXCL13-CXCR5 cell-based neutralization assay (Fig. 4D), which confirmed the improvements in potency over the parental 3B4 molecule.

To allow quantification of affinity improvements, BIAcore analysis was performed on the reformatted 3B4 variant scFv-Fc fusion proteins. Figure 5A shows representative traces for the parental clone 3B4 binding to both human and cynomolgus CXCL13 compared with optimized clones H6 (Fig. 5B) and E10 (Fig. 5C); a single concentration of 25 nM antigen is shown in each case for clarity. Kinetic analysis was performed for each of the top-performing clones, and this data are summarized in

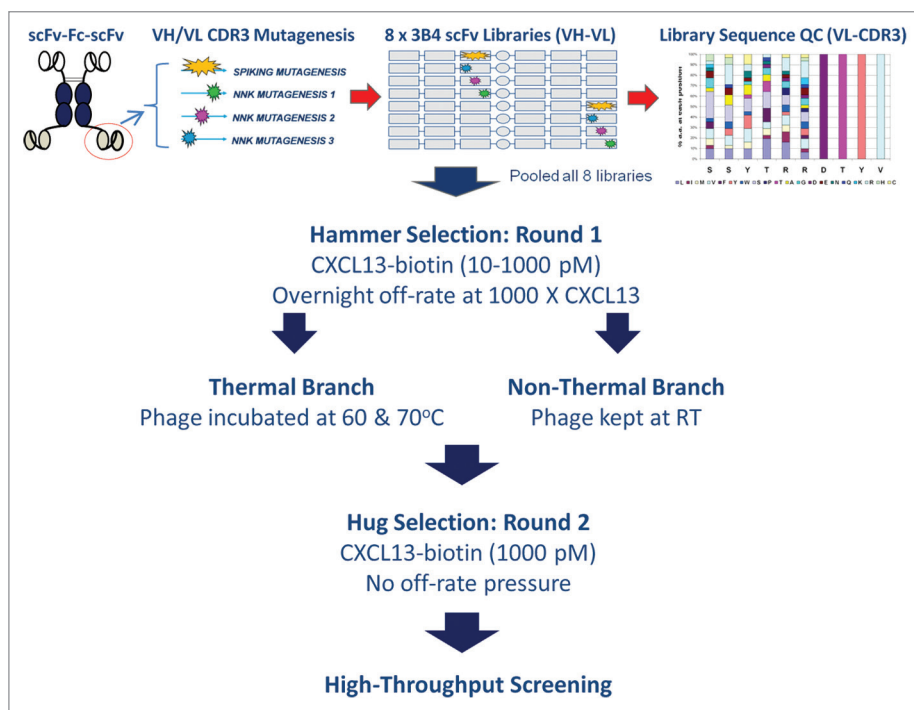


Figure 3. Schematic workflow for mutagenic library design, build, and selection.

Table 1. Across the final clone set, apparent K_D improvements of up to ~19-fold for human CXCL13 and 4 100-fold for cynomolgus CXCL13 were achieved.

Biophysical assessment of optimized 3B4 variants. Top-performing clones ranked on the basis of high-throughput HTRF competition assays and BIAcore affinity analyses were next triaged in a thermal ELISA. In this assay, a fixed concentration of each purified scFv-Fc was heated at 60 °C for 1 h, aggregated material was removed by centrifugation and the clarified supernatant was assayed for residual binding to antigen alongside an unheated control sample. Fold-change in EC_{50} between heated and unheated protein was compared for 3B4 and optimized 3B4 variants. Representative examples of this assay are shown comparing parental 3B4 (Fig. 6A), with optimized clone E10 (Fig. 6B). While 3B4 experiences a 40-fold loss in activity upon heating, E10 activity remains virtually intact under the same conditions. Fold-changes for the top clones selected on the basis of their performance against human and cynomolgus CXCL13 in this functional assay are summarized in Figure 6C. Under these assay conditions, all affinity-optimized clones were more stable than 3B4, independently of whether they were selected with (clones C7, H8, and E10) or without (clones C4, H6, A1) thermal challenge in round 2 of selection.

Importantly, clones that have been mutated away from wild-type sequence in the central combining site could potentially suffer loss of specificity in their target binding characteristics. In Figure 6D, cross-reactivity binding ELISA analyses are summarized, showing that the parental clone 3B4 and prioritized daughter clones A1, C4, and E10 show little or no unwanted binding to closely related CXCL-family chemokines, including murine

CXCL13. De-prioritized daughter clones A3 and E2 are shown for contrast (Fig. 6D), as they did show some moderate binding to mCXCL10.

To further characterize and rank our prioritized clones, more in-depth biophysical assessment was performed. We have previously shown that thermal melting curves generated using the fluorescent dye Sypro Orange correlate very well with traditional DSC methods, and this approach significantly minimizes protein usage while greatly increasing sample throughput.²¹ We used Sypro Orange to generate thermal transition points for our 3B4 scFv-Fc variants and this comparative analysis is shown in Figure 6E. While A1 and E10 (our best-behaved clones from the thermal ELISA) also have the highest T_m values, 3B4 appears more stable than clones H6, H8, and C4, despite the fact that H8 was selected from round 2 outputs subjected to thermal challenge at 70 °C.

The behavior of these scFv-Fc fusion proteins under conditions of thermal stress was also assessed using a forced aggregation assay. Proteins were prepared at 1 mg/ml and heated at various temperatures for a 24 h period. After this incubation, samples were analyzed by analytical SEC to determine the percentage of residual monomeric protein remaining (Fig. 6F). The same rank order of clones was observed in this assay with A1, E10, and C7 all showing more resistance to thermal stress than parental 3B4, but 3B4 was again more stable than H6, H8, or C4.

The thermal ELISA, T_m determination and forced aggregation assay all interrogate slightly different aspects of molecular stability. While the T_m is a dynamic real-time measurement of the mid-point of the thermal transition of the protein, both the thermal ELISA and forced aggregation assay are end-point snapshots of what, in reality, are complex reactions. In both cases, during the course of the assay incubations there will be dynamic protein unfolding and re-folding, as well as aggregation events, which reflect the inherent stability of the individual V_H and V_L domains and the stability of the interface between them. Aggregated protein arising from incubation at elevated temperatures is accounted for indirectly in the forced aggregation assay by reporting results on the basis of the percentage of monomer that remains. Discrepancies with this data and that observed in the thermal ELISA may well be due to lower level aggregates that are not efficiently removed by centrifugation at 14 000 $\times g$ and can still mediate antigen binding, thereby minimizing the apparent fold loss in activity.

To assess the relative outcomes of thermal challenge during selection, a random selection of 12 affinity-optimized clones from the 60 °C and 70 °C branches were compared in the thermal ELISA. We found that the average loss in activity for the 60 °C branch was 8-fold whereas this decreased to 4-fold for

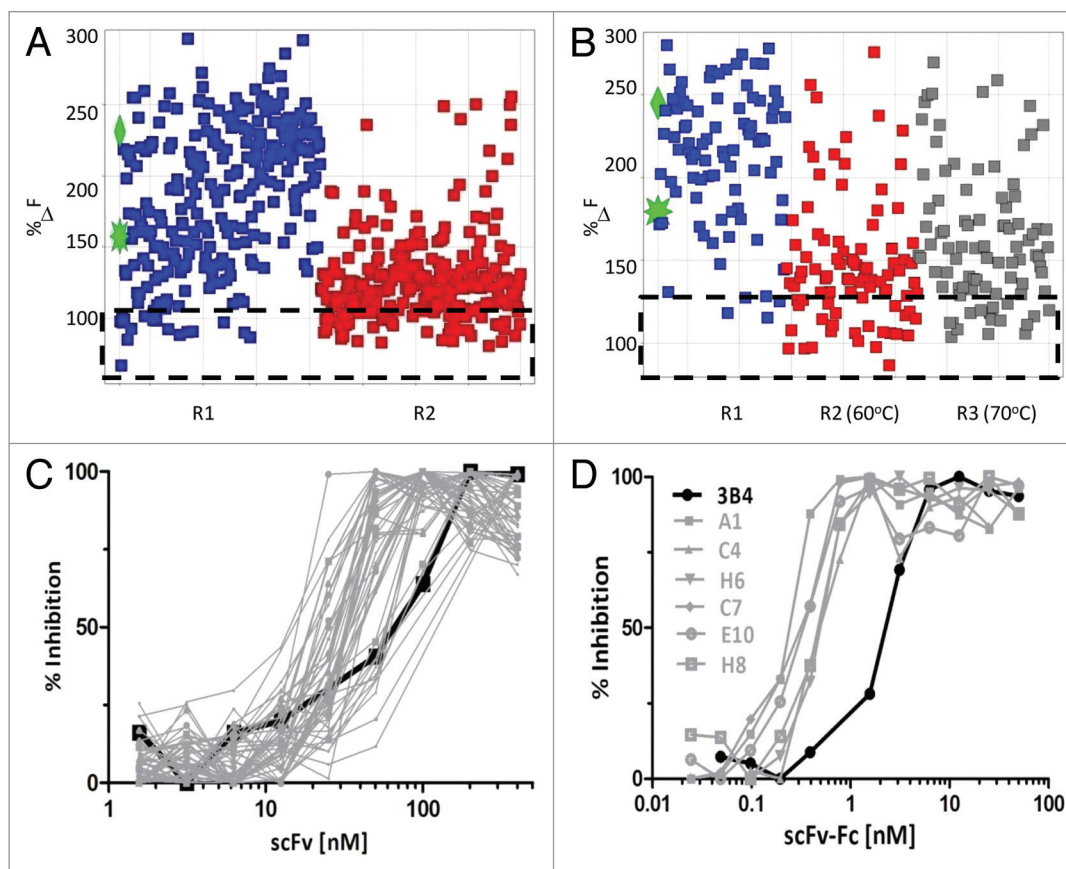


Figure 4. Workflow for the affinity, cross reactivity and stability engineering of the anti-CXCL13 clone 3B4. A high-throughput HTRF screen was performed on 500 randomly selected clones picked from two rounds of hammer-hug selection (A) and 176 clones picked from a hammer-hug style selection which incorporated a thermal challenge step of 60 °C and 70 °C (B). Changes in output fluorescence for mutated clones (blue, red and gray squares) were measured relative to wild type 3B4 (green star) and a negative control scFv (green diamond). The top performing 3B4 variants (boxed populations) were purified as scFvs and triaged in a cell based HTRF-IP-1 neutralization assay relative to wild type 3B4 scFv (C). The most potent 3B4 scFv variants were subsequently reformatted to scFv-Fc fusion, expressed, purified and re-ranked in the HTRF-IP-1 assay (D).

the 70 °C branch. There was also a much broader range in fold losses at the lower temperature (4.5–14 at 60 °C vs. 2–6 at 70 °C, data not shown). This suggests that thermal challenge certainly biases the population toward higher thermal stability; however, our triaged clones were prioritized first on the basis of significant improvements in affinity and potency and only secondarily for their stability. The complex nature of the optimization undertaken, coupled with our primary focus on affinity, resulted in some leads with exemplary potency, but only marginally (or not at all) improved stability. Notwithstanding this, the relatively high-throughput nature of the thermal ELISA in comparison to DSC made it a useful tool to assess the stability of our affinity matured clones at an early stage of screening and allowed us to prioritize clones for more in-depth biophysical analysis. It is clear from the differences in rank order of clones across the biophysical assays used that a multi-parametric approach is required to identify clones that are definitively improved in both stability and solubility. Using this combination of biophysical assays allowed us to prioritize clones A1 and E10, which performed significantly better than 3B4 under all conditions tested (comparative data summarized in Table 1).

Characterization of reformatted lead scFv-Fc-scFvs. Expression and purification analysis indicated that the reformatted scFv-Fc-scFvs were expressed at similar levels to their composite binding domains formatted as IgGs. Small-scale transient expressions (< 10 L) were performed in 293 cells to enable side-by-side comparisons of IT1 and E10 domains reformatted individually as IgGs or in an IT1-Fc-E10 bispecific molecule. Our bifunctional molecules were expressed at 20–30 mg/L, a level that compares favorably with typical IgG1 antibody molecules, which express in the range of 20–50 mg/L in our hands under the same conditions (data not shown). All 3 molecules expressed at similar levels and were purified in a standard monoclonal antibody workflow using ProA and preparative SEC. The scFv-Fc-scFv process was shown to be scalable up to 300 L. Representative purified samples are shown in Figure S1.

Functional analysis indicated that C-terminal linkage of the anti-IT1 scFv in the bifunctional format had a negative effect on function while the CXCL13 scFv behaved similarly in both N- and C-terminal orientations. For this reason, all subsequent molecules were constructed with CXCL13 variants at the C-terminus. Reformatted scFv-Fc-scFvs containing

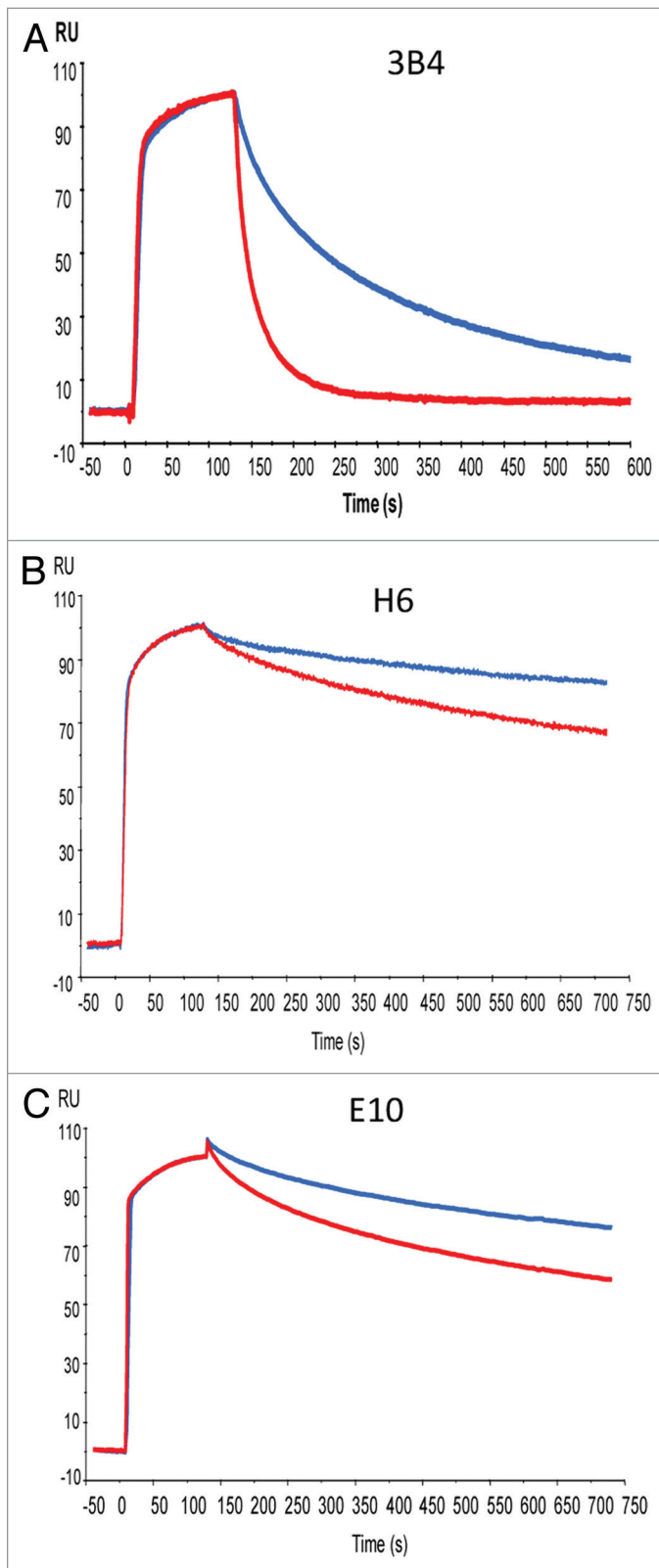


Figure 5. Comparative kinetic analysis of 3B4 variants with human- and cynomolgus-CXCL13. Overlaid and normalized BIAcore sensorgrams for the interaction of 3B4, H6 and E10 scFv Fc-fusion proteins with 25 nM human-CXCL13 (blue) and cynomolgus-CXCL13 (red), demonstrating significant improvements in off-rate post-optimization.

affinity optimized anti-CXCL13 domains were recharacterized for CXCL13 binding. In this format K_D values of 800 pM, 10 pM, and 67 pM were obtained for IT1-Fc-3B4, IT1-Fc-A1, and IT1-Fc-E10, respectively. These values correlate well with those obtained for the same domains in scFv-Fc format, being within 2-fold of those previously determined (shown in Table 1). Moderate differences in K_D measurements are most likely driven primarily by the slightly altered presentation of the scFv when at the C-terminus of the Fc.

In addition to manufacturability, formulation of complex bi-specific molecules can be challenging. In our case, we were aiming for subcutaneous administration, which requires high stability, low aggregation at high concentration and low viscosity. An early IT1-Fc-3B4 bispecific molecule that demonstrated poor thermal stability (Fig. 2B) also performed poorly in formulation tests. This scFv-Fc-scFv was concentrated to 50 mg/ml in a series of standard formulation buffers ranging from pH 4.5 to 7.5. Aliquots of this sample were stored at room temperature (RT) and 4 °C over a period of 5 weeks, and sampled at time zero and after each subsequent week to measure the percentage of aggregated material by analytical SEC. The initial molecule had high levels of aggregation at day 0 in all buffers tested and this deteriorated over time with up to 50% aggregation measured at pH 7.5 after 5 weeks at 4 °C (Fig. 7A).

The reformatted scFv-Fc-scFvs with anti-IT1 at the N-terminus and either A1 (Fig. 7B) or E10 (Fig. 7C) at the C-terminus were tested under similar conditions at 100 mg/ml for 6 weeks or 7 weeks, respectively. Figure 7 demonstrates very clearly that scFv-Fc-scFvs containing optimized anti-CXCL13 domains A1 and E10 perform significantly better than those with the 3B4 parental molecule. It is notable that the scFv-Fc-scFv containing the E10 domain in particular, which was selected and screened under conditions of thermal stress, shows minimal aggregation when stored long-term at 100 mg/ml at 4 °C in all buffers tested.

A further consideration for subcutaneous dosing is the potential for prohibitive viscosity in high concentration protein solutions. Our lead IT1-Fc-E10 bispecific molecule was formulated at a range of concentrations and its viscosity compared with that of 3 internal human IgG1 antibodies expressed, purified, and formulated under standard conditions.²¹ The scFv-Fc-scFv performed similarly to these representative antibodies, with viscosity remaining < 15 cP for the highest concentration tested (130 mg/ml). These results are summarized in Figure 8.

Discussion

In recent years, the molecular engineering of antibodies has progressed considerably, but the generation of highly functional, clinically viable, bispecific molecules containing scFvs remains a challenge.³ The heterogeneous nature of antibody v-domain solubility, stability and pairing affinity characteristics means that each v-domain pair must often undergo a bespoke engineering process to be suitable for inclusion in a final bispecific molecule.^{1,12} Indeed, the majority of studies published so far have described significant efforts just to make constructs containing

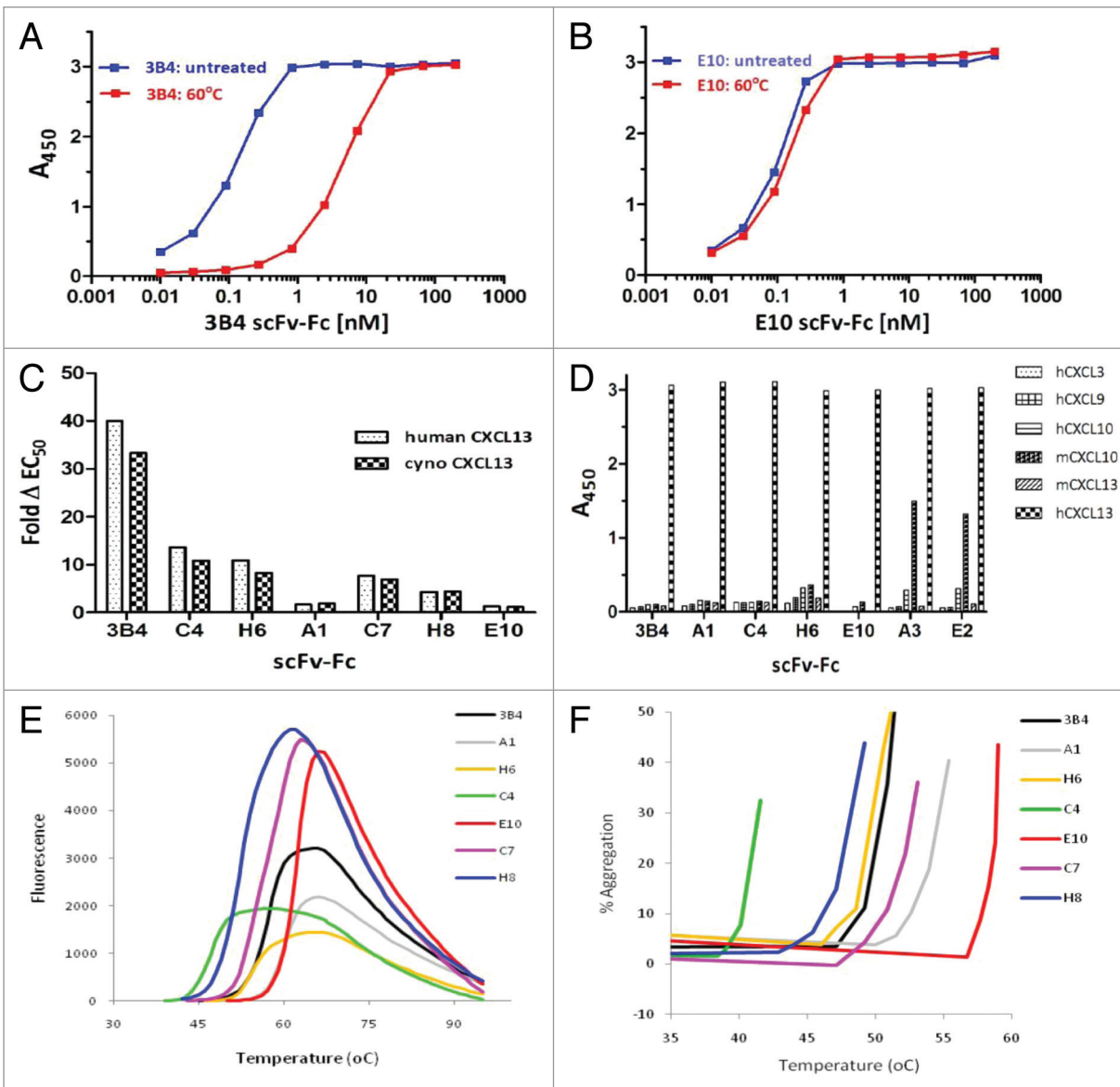


Figure 6. Biophysical and specificity assessments of affinity matured anti-CXCL13 scFv-Fc fusions by thermal ELISA. **(A)** 3B4 and the affinity matured variant E10 **(B)** were ranked in a thermal ELISA stability assay with the blue and red curves representing unheated and heated parental scFv-Fc fusions, respectively. **(C)** The fold loss in human CXCL13-binding ability is indicated by ΔEC_{50} and these values compared for representative clones on both human and cynomolgus CXCL13. **(D)** Anti-CXCL13 scFv-Fc fusions at 100 nM were tested for binding to closely related, similarly positively charged chemokines: human CXCL3/9/10/13 and mouse CXCL10/13. Deprioritized clones A3 and E2 are included as examples where moderate cross-reactivity to CXCL10 was observed at high concentration. **(E)** Sypro orange stability analysis for all prioritized clones and parental 3B4. **(F)** Forced aggregation analysis for all prioritized clones and parental 3B4.

scFvs that can be expressed and purified in a manner that is acceptable for manufacturing, with the goal being a product suitable for dosing intravenously at low concentrations.^{2,11,14} For scFv-containing molecules to function in the more challenging, high-concentration, subcutaneous dosing setting, the solubility, and stability of the molecules must be exemplary.

The structural design of bispecific molecules can have a strong influence on their functional characteristics, so the current study began with the exploration of scFv-Fc-scFv molecules composed of proof-of-concept binding domains in combination with different C-terminal linkers. We compared a conventional flexible

(G₄S)₃ linker to the structurally similar (A₄T)₃ and also included a charged linker (CL), modified from that described by Chaudhary and coworkers.²² The linkers were positioned between the C-terminus of a human scFv-Fc (IgG1 Fc) and the N-terminus of the second scFv domain, and the resulting constructs were tested in dual binding, stability, and rat PK analyses. All three linker variants demonstrated favorable dual antigen binding and stability characteristics along with PK behavior comparable to standard monoclonal antibodies. Based on its structural simplicity, the (A₄T)₃ linker was therefore chosen for further study and combined with therapeutically relevant

Table 1. Biochemical and biophysical properties of anti-CXCL13 scFv-Fc clones

Clone	Thermal	VL-CDR3 ^a	CXCL13	k_a (M ⁻¹ s ⁻¹)*	k_d (s ⁻¹)	KD (pM) ^b	Fold-gain in stability over 3B4 ^c
3B4	-	SSYTRRDYV	Human	3.24×10^7	0.0121	371.5	-
			Cyno	1.63×10^6	0.0610	37330.0	-
A01	No	ASTTLFDYV	Human	9.28×10^6	0.0003	29.82	23.5
			Cyno	7.65×10^6	0.0005	65.90	17.5
H06	No	ASVVVTDYV	Human	7.54×10^6	0.0003	37.58	3.7
			Cyno	7.82×10^6	0.0007	88.91	4.0
C04	No	SSAGIISVYV	Human	6.22×10^6	0.0003	46.04	2.9
			Cyno	7.51×10^6	0.0006	77.63	3.1
E10	Yes:70 °C	ASATLLDYV	Human	9.81×10^6	0.0005	45.44	30.8
			Cyno	2.16×10^7	0.0021	8.98	27.8
H08	Yes:70 °C	TSVTVEDYV	Human	8.53×10^6	0.0002	19.91	9.3
			Cyno	6.89×10^6	0.0003	47.41	7.6
C07	Yes:70 °C	SSPTFTEPYV	Human	8.03×10^6	0.0002	27.89	5.2
			Cyno	1.11×10^7	0.0005	46.31	4.8

^aVL CDR3: All beneficial mutations were localized to VLCDR3. ^bAffinity constants were determined by 1:1 global-fit analysis of the binding curves. All of the sensorgram data fitted well to the 1:1 interaction models and χ^2 values for all analyses were < 1.0. ^cOn-rates (K_A) are approaching the maximum measurable value; therefore the K_A and K_D values should be considered “apparent” and not absolute values. ^dFold gains as determined by thermal ELISA.

scFvs targeting CXCL13 and a cell-surface expressed immune target in an scFv-Fc-scFv format for bispecific immune-modulatory applications.

The structural stability and solubility of the scFv modules themselves are also critical features of scFv bispecific molecules. We hypothesized that native human scFvs (i.e., isolated in that format, rather than converted from humanized monoclonal antibodies,² or from pools of human Fab fragments^{10,11}) might be the best source of molecules that would function well in this setting, with the minimum requirement for stability engineering. Our findings suggest that, in the case of our anti-IT1 domains, this was indeed true because the primary domains exhibited high thermal stability, solubility, and low aggregation at high concentration, without any need for secondary engineering. On the contrary, preliminary analyses indicated that, although the lead CXCL13 scFv 3B4 was a potent neutralizer in an in vitro CXCR5-dependent signaling assay, it had a relatively fast off-rate for human CXCL13, poor cross-reactivity with cynomolgus CXCL13 and was associated with low thermal stability in early scFv-Fc-scFv formats.

To ameliorate these issues with 3B4, all three sub-optimal properties of the parental scFv were addressed in a single CDR-based mutagenesis and re-selection approach in which the CDR3 region of either the V_L or V_H chain was randomized, with frameworks left untouched. The resulting phage-displayed scFv libraries were selected using a pragmatic adaptation of the theoretical methods described by Zahnd et al.,²³ which we have dubbed the “Hammer-Hug” method. This method applied a highly stringent first round of selection (Hammer) using low concentrations of biotinylated antigen, coupled with an aggressive overnight off-rate competition using high concentration unlabeled antigen. This round attempts to drive the selection conditions to specifically enrich only those clones

having off-rates in the low pM range. A rescue round (Hug) was then performed at moderate antigen concentration in the absence of off-rate competition and in the presence or absence of thermal challenge. Selected outputs from both rounds were ranked for neutralization potency, affinity for human and cynomolgus CXCL13 and performance in thermal ELISA. These analyses showed that the method was extremely efficient at selecting clones with dramatically improved affinity and stability. That we were able to isolate clones of improved stability both with and without thermal challenge during library selections suggested that the method intrinsically selected for improved v-domain pairing. It is notable that the most stable anti-CXCL13 clone (E10) was indeed isolated from the thermally-selected branch.

Importantly, we observed considerable sequence diversity in the affinity-improved population. This suggests that, at least in this case, the stringency of the selections did not have the diversity-limitation effect predicted in silico.²³ Sequencing of our lead panel revealed that optimized clones were exclusively mutated in V_L -CDR3, suggesting sub-optimal V_H - V_L pairing in the parental scFv. Lead mutants were subsequently subjected to small-scale biophysical assessment of T_m and aggregation propensity. High-performing clones were reformatted into scFv-Fc-scFvs in combination with lead IT1 scFvs and re-characterization demonstrated maintenance of dual functionality and favorable biophysics at 1 mg/ml scale. Expression characteristics of lead scFv-Fc-scFvs in transient HEK or stable CHO were similar to the parental molecules expressed as IgGs. Most importantly, the scFv-Fc-scFvs were purified in a standard mAb process amenable to scale-up and manufacture, and further biophysical analysis demonstrated stability over a 50-d period at 100 mg/ml in standard pharmaceutical buffers with less than 2% aggregated species and a viscosity of less than 15 cP.

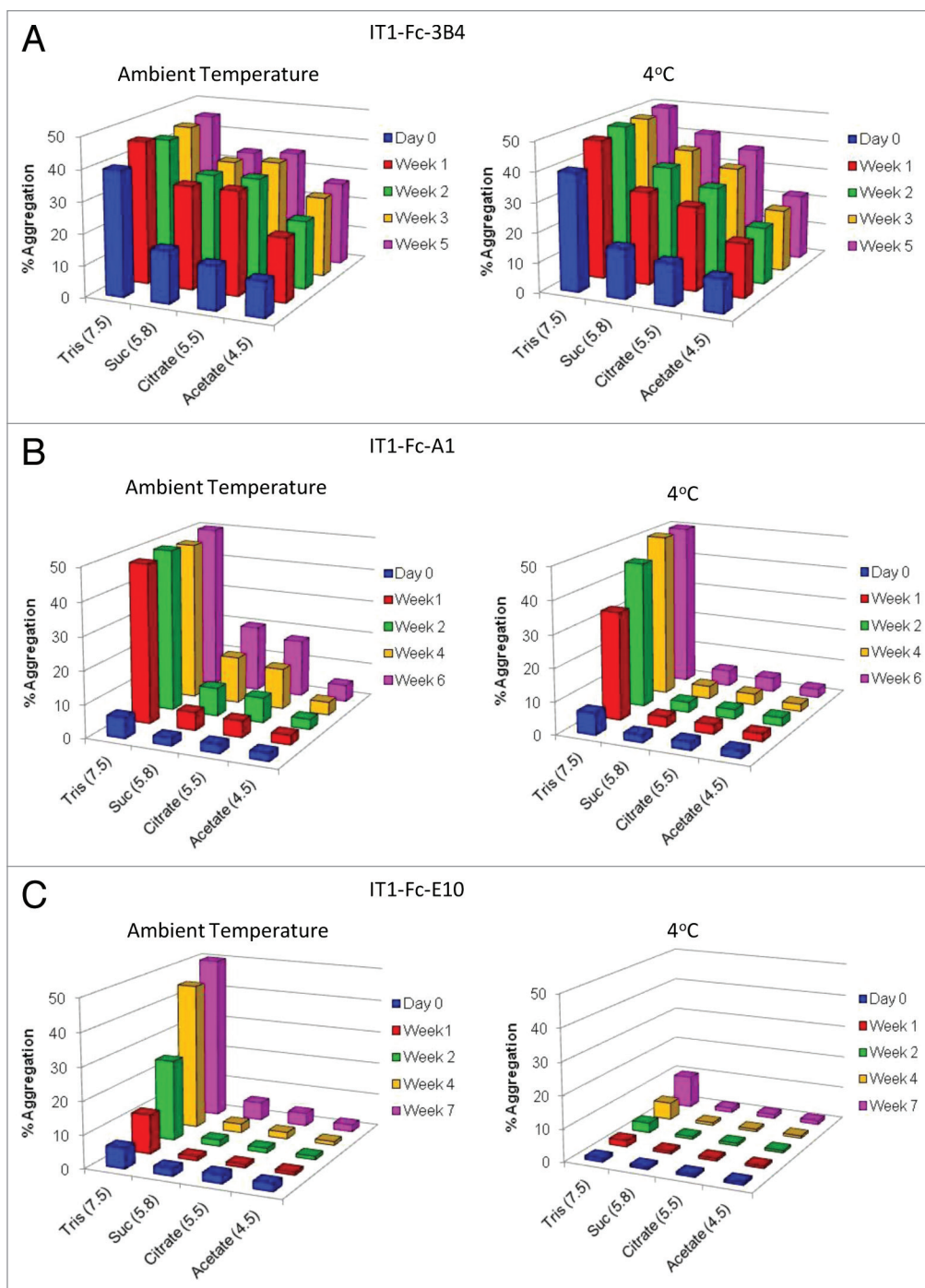


Figure 7. High Concentration Formulation Analysis of Reformatted scFv-Fc-scFvs. Reformatted scFv-Fc-scFv bispecific molecules incorporating (A) 3B4, (B) A1, and (C) E10 were formulated to high concentration (50 mg/ml for 3B4, 100 mg/ml for A1 and E10) in a variety of standard buffers at varying pH and monitored for aggregate formation over a period of 5–7 weeks after incubation at ambient temperature and 4 °C.

In summary, this study demonstrated for the first time that simplified bispecific antibodies based on the scFv can be engineered to have genuine potential in highly challenging dosing scenarios. The data presented here is strongly suggestive that the isolation, engineering, and testing of human antibody v-domains for such molecules should be performed in the scFv format, rather than re-purposed from elsewhere.

Materials and Methods

Design, expression, and purification of POC scFv-Fc-scFv constructs. A set of three DNA sequences were designed to introduce the linkers at the desired positions and generate intermediate constructs for subcloning. The N-terminus of the fragments utilized a naturally-occurring *Bsr*GI site within the human IgG1-derived

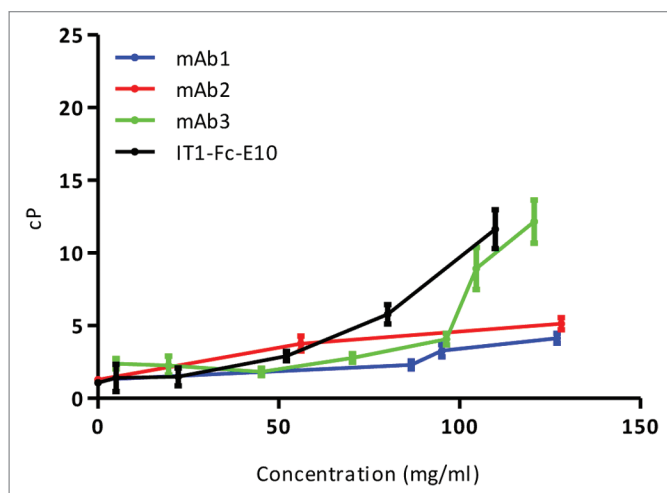


Figure 8. Lead IT1-Fc-E10 exhibits mAb-like viscosity. At concentrations higher than 100 mg/ml, the bispecific exhibits viscosity of <20 cP, beyond which fine-needle injection becomes difficult due to back-pressure. Control hlgG1 mAbs 1, 2, and 3²¹ are included for reference, having been expressed, purified and formulated in the same buffer as the bispecific.

CH3 region, and a *NotI* restriction site was added to the C-terminus of all three linkers, encoding three alanine residues. The three linker amino acid sequences (A4T, G4S, and CL) that were positioned at the C-terminus of the human CH3 region were as follows (residues encoding the *NotI* site are underlined): A4T: TAAAATAAAA TAAAATAAAA; G4S: GGGGSGGGGS GGGGSAAA; CL: EGKSSGASGE SKVDAAA. Additional cloning sites (*FseI* and *EcoRI*) downstream of the *NotI* site were included to permit subcloning of C-terminal binding domains. DNA synthesis of these intermediate fragments was performed by GeneArt (Invitrogen). An scFv that had previously been isolated against FITC-BSA from an in-house human phage display library was subcloned into each of the three intermediate constructs as a *NotI-FseI* fragment. Subsequently, the three *BsrGI-FseI* fragments containing a C-terminal portion of the human CH3 region, the linker sequence (A4T, G4S, or CL), and the anti-FITC-BSA scFv were individually subcloned into a mammalian expression vector containing an anti-human TNF scFv (isolated as for FITC-BSA scFv) fused to human CH2 and CH3 regions via a modified human IgG1 hinge region. The final constructs contained the anti-TNF scFv, fused to a human hinge and CH2-CH3 regions, followed by the linker of interest and the anti-FITC-BSA scFv. All scFv-Fc-scFv proteins were expressed transiently in 293 cells using standard methods. Conditioned media was harvested 5 d post-transfection, clarified by centrifugation and filtration at 0.22 μ m and batch purified using ProSep Ultra Plus (Millipore). Eluted proteins were dialysed against 1 \times PBS pH 7.4.

Dual specificity binding ELISA. Nunc MaxiSorp F96 plates were coated with FITC-BSA (Sigma, A9771) at a concentration of 1 μ g/ml in 1 \times PBS (pH 7.2) at 37 $^{\circ}$ C for 1 h. Plates were washed 4 times with 1 \times PBS containing 1% (v/v) Tween 20 on a Titertek Zoom plate washer. Wells were blocked with 200 μ l

PBS containing 2% (w/v) milk at 37 $^{\circ}$ C for 1 h, and then washed as before. Dilutions of scFv-Fc-scFv protein samples in 1 \times PBS were added as indicated (100 μ l per well) and incubated at RT for 1 h. The plates were washed as before, biotinylated human TNF (1 μ g/ml, eBioscience) in 1 \times PBS was added, and incubated at RT for 1 h. Following washing as before, streptavidin-HRP (R&D Systems) was added and incubated for 1 h at RT. After final washing, SureBlue TMB substrate (Kirkegaard and Perry Laboratories) was added for 15 min at RT and the reaction stopped with 1 M sulfuric acid. Absorbance at 450 nm was measured using an Envision 2104 Multilabel plate reader (Perkin Elmer).

DSC. Thermal stabilities of scFv-Fc and bispecific antibodies were analyzed using MicroCal capillary DSC system equipped with an autosampler. Samples at 0.3 mg/ml in PBS, pH 7.2 were heated from 10 to 100 $^{\circ}$ C at a scan rate of 100 $^{\circ}$ C/h. The resulting heat capacity was baseline corrected by subtracting a PBS buffer scan and fitted to 3 or 4 non-2 state transitions using Origin7.0 software from MicroCal (OriginLab Corporation).

Forced aggregation analysis. Protein samples at 1 mg/ml in PBS were placed in a 96-well optical reaction plate (Applied Biosystems), covered with 40 μ l of mineral oil (Sigma-Aldrich), and sealed with an adhesion film (Applied Biosystems). The plate was placed in a PCR block heater (Peltier Thermal Cycler DNA Engine DYAD, Bio-Rad) with a constant temperature gradient ranging from 40 to 64 $^{\circ}$ C. After 24 h incubation, 10 μ l of each of the heated samples, as well as a control sample kept at 4 $^{\circ}$ C, were analyzed on an Agilent 1200-series HPLC (Agilent Technologies), with a QC-PAK-GFC300 column (Tosoh Bioscience LLC), and PBS as running buffer. For each sample, the percent aggregate was calculated as the ratio of remaining bispecific molecule peak area at each temperature to peak area of the 4 $^{\circ}$ C control sample.

High concentration protein solubility study. Bispecific protein solubility was assessed at 50 mg/ml for 3B4 parental molecule and at 100 mg/ml for affinity matured A1 and thermally challenged E10 molecules. Each protein was buffer exchanged into four formulation buffers (Tris at pH 7.5, succinate at pH 5.8, citrate at pH 5.5 and acetate at pH 4.5) using 10K molecular weight cutoff dialysis cassettes (Thermo Scientific). The dialyzed protein solutions were concentrated to the final target protein concentration with Ultracel microcentrifuge concentrators (Millipore) and protein concentrations were determined using a Nanodrop2000 Spectrophotometer (Thermo Scientific). The buffered protein samples were incubated at ambient temperature and 4 $^{\circ}$ C up to seven weeks. At each time point, the incubated samples were analyzed on Agilent 1200 HPLC system with QC-PAK-GFC300 analytical size exclusion chromatography column and PBS supplemented to 400 mM NaCl as running buffer.

DLS-based viscosity analysis. Bispecific protein samples formulated in the succinate buffer were prepared at 0–110 mg/ml. Viscosity analysis was performed on a 1536-well plate (VWR) with 8 μ l of protein sample and 0.5 μ l of a diluted nanosphere tracer bead mixture added to each well. The 300 nm diameter nanosphere bead (Thermo Scientific) was diluted 10-fold into the

succinate formulation buffer prior to use. After a brief centrifugation to remove air bubbles, the plate was placed in DynaPro Plate Reader DLS system (Wyatt Technology) for DLS measurement. Nanosphere size measurements were analyzed using the Dynamics software provider by Wyatt Technology and as described by He et al.²⁴

Rat PK study. Nine healthy adult female CD rats (Charles River), weighing about 350 g were used in the PK study. The animals were housed individually, with free access to food and water. The scFv-Fc-scFv proteins were all diluted to a concentration of 1 mg/ml in sterile PBS (pH 7.2), and administered to the rats at a dose of 1 mg/kg by intravenous injection via the tail vein. Blood samples were taken at the indicated post-dose time intervals from the rats via manual tail vein sampling into heparinized tubes. Plasma was collected from the samples by centrifugation at 3 000 g for 10 min, transferred into new tubes and stored at -20 °C for subsequent analysis by ELISA (see below). PK parameters were calculated using WinNonLin version 5.2 (Pharsight).

Nunc Maxisorp plates were coated with FITC-BSA (Sigma) or recombinant human TNF (R&D Systems) at 1 µg/ml in sodium carbonate buffer, pH 9.6. Plates were blocked with Superblock (Pierce) for 1 h. Samples were prepared at 1:100 in dilution buffer (in PBS/1% (v/v) Tween-20/1% Superblock) and calibrants were prepared by diluting each scFv-Fc-scFv stock in a 3-fold dilution series from 1000 ng/ml in dilution buffer containing 1% rat plasma. Assay plates were washed 4 times with PBS/Tween on a Biotek plate washer and 100 µl of calibrant or diluted sample were added in duplicate at RT for 1 h. The plates were washed an additional 4 times and detection of human Fc domains was achieved using an anti-human IgG/HRP conjugate (binding site) diluted in dilution buffer (1:50000 for FITC-BSA assay, 1:75000 for anti-TNF). The plates were washed 4 times with PBS/Tween and developed with Ultra TMB (Thermo) followed by 2 M sulfuric acid. Absorbance at 450 nm was measured using a Molecular Devices M5 plate reader.

Mutagenesis and construction of phage libraries. 3B4 mutant sub libraries were constructed via splice-overlap-extension (SOE)-PCR, with mutation being introduced into V_H-CDR3 or V_L-CDR3. Two types of mutagenesis were employed in each case, the first involving NNK degenerate codons and the second involving custom-designed soft randomization degenerate primers. The NNK degenerate codons targeted the CDR3 region of either the V_H or V_L chain via the use of 3 overlapping 6-mers, resulting in 3 NNK mutant sub-libraries for both the V_L and the V_H chain. The soft randomization approach targeted the full length of the CDR3 region, where 50% wild-type sequence and 50% random sampling were allowed at each position. Therefore, 8 sub-libraries were constructed in total, 6 NNK mutant libraries and 2 soft mutant libraries targeting the CDR3 of either the V_H or V_L chain. Construction of the mutant libraries was performed as described previously.^{19,25} Primary and secondary SOE-PCRs were performed using Platinum® Taq DNA Polymerase High Fidelity (Invitrogen), according to the manufacturer's recommendations. SOE-PCR products were restriction digested, purified, and cloned into the pWRIL-1 vector in *E. coli* TG1 as described previously.²⁶

Phage library rescue and selections. Rescue of the 8 sub-libraries was performed as previously described.²⁶ An equal volume of each of the 8 resultant precipitated phage pools were combined to produce a single master phage pool. An initial two round solution-phase selection approach included a high stringency off-rate selection first round and a less stringent (no off-rate selection) second round. We termed this style of selection "Hammer-hug" and it builds on theoretical methodology described by Zahnd et al.²³ Round 1 was divided into three branches (A, B, and C), corresponding to biotinylated hCXCL13 (b-hCXCL13) selection concentrations of 1000 pM, 100 pM, and 10 pM, respectively. Round 1 "off-rate" competition was achieved by adding up to 1000-fold excess of non-biotinylated hCXCL13 overnight at 4 °C. Round 2 selected all three Round 1 outputs on 1000 pM biotinylated-hCXCL13. In both rounds, we included calf thymus histones (Sigma-Aldrich) at 10 µg/ml in blocking buffer as a deselection agent.

An alternative Round 2 (Round 2a) was also performed to incorporate a thermal shock step prior to selection of the phage, an approach previously described.²⁷ In this case, all Round 1 output pools were combined at the phage precipitation step and heated to either 60 °C or 70 °C for 15 min. Following thermal shock, the two pools were cooled on ice for 10 min, centrifuged, and the resultant phage supernatants blocked with 3% M-PBS (containing 10 µg/ml Histones) for 1 h at RT. Both blocked phage pools were selected against 1000 pM biotinylated-CXCL13 as before.

ScFv and scFv-Fc expression and purification. Small-scale, single-step scFv purifications from periplasmic extracts were performed for more detailed HTRF and Tb IP-One HTRF titration analysis using His-Select 96-well plates (GE Healthcare) as described previously.²⁸ ScFv-Fc fusion proteins were expressed transiently in COS cells and purified from filtered conditioned medium using ProPlus tips from Phynexus on the automated Phynexus MEA.

HTRF assay. A high-throughput competition HTRF assay was established to facilitate the identification of affinity improved clones. The wild type IgG 3B4 was labeled with europium cryptate using a cryptate labeling kit (CisBio) according to manufacturer's instructions. The final assay mixture consisted of 0.8 nM biotinylated human CXCL13 (PeproTech), 1/400 dilution of europium cryptate labeled 3B4, 1/2000 dilution of SA-XL665 (CisBio), and 1% (v/v) periplasmic extract containing the scFvs of interest in a total reaction volume of 20 µl in 1x assay buffer [50 mM sodium phosphate, pH 7.5, 400 mM potassium fluoride, and 0.1% BSA (w/v)]. The assay was performed and output data plotted as previously outlined.²⁵ For the HTRF analysis of clones of interest purified as scFv, the assay was repeated as above using purified scFv (250–0.0014 nM) and resulting data was compared with that of the parental scFv 3B4.

Human CXCL13 Tb IP-One HTRF assay. A cell based neutralization assay was developed using the Cisbio IP-One HTRF Kit according to the manufacturer's recommendations. Stably-transfected HEK293:Gqi/hCXCR5 cells were plated at 10,000 cells/well in fresh DMEM high glucose medium containing 10% (v/v) heat-inactivated fetal bovine serum (Hyclone), 2 mM Glutamax, 0.75 mg/ml Puromycin (Sigma), and

0.75 mg/ml G418 (Sigma) in 384-well poly-D-lysine coated solid white plates (BD Biosciences). Plates were incubated overnight at 37 °C/5% CO₂. The following day, 5 nM human CXCL13 in 1× IP-one stimulation buffer (CisBio) containing 0.5% BSA (v/v) was added to a dilution series of scFv-Fc fusions prepared in 1× MOPs buffer (24 mM MOPS; 0.3 mM EDTA; 300 mM sorbitol). This was incubated at RT for 30 min, and 20 µl of the scFv-Fc/CXCL13 mixture was then added to the cells and incubated at 37 °C, 5% CO₂ for 90 min. After addition of IP1-d2 and anti-IP1-Tb cryptate, the plates were incubated at RT for 1 h and then read on an EnVision Multi Plate Reader (Perkin-Elmer) with excitation at 340 nm and two emission readings at 620 nm and 665 nm. All readings were expressed as a change in fluorescence (%ΔF), and all data was normalized and plotted as percent inhibition using Prism 5 software (Graph Pad).

Thermal stability ELISA. Maxisorp plates (Nunc) were coated with 1 µg/ml human or cynomolgus CXCL13 in PBS overnight at 4 °C. Wells were washed three times with 300 µl of PBS containing 0.05% (v/v) Tween-20, and blocked in 200 µl of blocking buffer (PBS/3% (w/v) milk with 1% BSA (w/v)) for 1 h. scFv-Fc fusion proteins were diluted to 200 nM in PBS, aliquoted into two fractions with one incubated on ice and the other at 60 °C in a thermocycler (Bio-Rad) for 1 h. After incubation, samples were centrifuged at 14 000 × *g* and supernatants used to prepare a 3-fold dilution series (200–0.01 nM) in blocking buffer that was then added to the CXCL13-coated plates for 1 h at RT. After extensive washing the plates were incubated with an anti-human-Fc (Pierce) for 1 h followed by further washing. The reaction was developed by addition of 75 µl per well of UltraTMB (Pierce) and stopped by addition of an equal volume of 0.18 M phosphoric acid. The plates were read in an Envision Multiplate reader at 450 nm. Data was plotted using Prism 5 software (Graphpad).

Off-target ELISA. Maxisorp plates (Nunc) were coated with 1 µg/ml of human CXCL3, 9, and 10, and murine CXCL10 and 13 (R&D Systems) in PBS overnight at 4 °C. Wells were washed three times with 300 µl PBS with 0.05% (v/v) Tween-20, and blocked in 200 µl of blocking buffer (PBS/3% [w/v] milk; 1% BSA [w/v]) for 1 h. ScFv-Fc fusion proteins were diluted in a 2-fold dilution series from 100–0.2 nM in PBS in blocking

buffer which were then added to the various CXCL-coated plates for 1 h at RT. Plates were developed as described in the section above. For clarity A₄₅₀ readings for only 100 nM of each scFv-Fc fusion binding to each of the CXCL proteins was plotted using the Prism 5 Software.

Biacore analysis of binding kinetics. Biacore analysis was performed using a T-200 biosensor, series S CM5 chips, an amine-coupling kit, 10 mM sodium acetate immobilization buffer pH 5.0, 1× HEPES-buffered saline EDTA-phosphate (HBS-EP) running buffer containing an additional 250 mM NaCl (final NaCl concentration 400 mM), and 3 M MgCl₂ (regeneration solution) (GE Healthcare). For the calculation of the kinetic constants for the interaction of scFv-Fc fusion with human/ cynomolgus CXCL13, approximately 8000 RUs of an anti-human IgG Fc (GE Healthcare) was covalently immobilized to flow cells 1 and 2 of the CM5 chip at pH 5.5. Then, 50–100 RUs of 3B4/3B4 variant scFv-Fc fusion (diluted in 1× running buffer) were captured on flow cell 2. Human or cynomolgus CXCL13 (100–25 nM) diluted in running buffer was flowed across both flow cells at 100 µl/min with a contact phase of 120 s and a dissociation phase of 600s, followed by a 5 s regeneration pulse with 3 M MgCl₂. All experiments were performed at 37 °C. For all experiments, the experimental data was corrected for instrument and bulk artifacts by double referencing²⁹ a surface immobilized with capture antibody without scFv-Fc-scFv using Scrubber version 2.0c software (BioLogic Software). The transformed data were fit to a 1:1 binding model in Biacore T200 evaluation software v1.0 (GE Healthcare) that includes a parameter for mass transfer.³⁰

Disclosure of Potential Conflicts of Interest

No potential conflicts of interest were disclosed.

Acknowledgments

We would like to thank Fionnuala McAleese, Adam Root, and Angela Widom for early work on scFv domain discovery.

Supplemental Materials

Supplemental materials may be found here: www.landesbioscience.com/journals/mabs/article/26201

References

- Chan AC, Carter PJ. Therapeutic antibodies for autoimmunity and inflammation. *Nat Rev Immunol* 2010; 10:301-16; PMID:20414204; <http://dx.doi.org/10.1038/nri2761>
- Miller BR, Demarest SJ, Lugovskoy A, Huang F, Wu X, Snyder WB, Croner LJ, Wang N, Amatucci A, Michaelson JS, et al. Stability engineering of scFvs for the development of bispecific and multivalent antibodies. *Protein Eng Des Sel* 2010; 23:549-57; PMID:20457695; <http://dx.doi.org/10.1093/protein/gzq028>
- Xu L, Kohli N, Rennard R, Jiao Y, Razlog M, Zhang K, Baum J, Johnson B, Tang J, Schoeberl B, et al. Rapid optimization and prototyping for therapeutic antibody-like molecules. *MABS* 2013; 5:237-54; PMID:23392215; <http://dx.doi.org/10.4161/mabs.23363>
- Bargou R, Leo E, Zugmaier G, Klinger M, Goebeler M, Knop S, Noppeney R, Viardot A, Hess G, Schuler M, et al. Tumor regression in cancer patients by very low doses of a T cell-engaging antibody. *Science* 2008; 321:974-7; PMID:18703743; <http://dx.doi.org/10.1126/science.1158545>
- Topp MS, Gökbuget N, Zugmaier G, Degenhard E, Goebeler ME, Klinger M, Neumann SA, Horst HA, Raff T, Viardot A, et al. Long-term follow-up of hematologic relapse-free survival in a phase 2 study of blinatumomab in patients with MRD in B-lineage ALL. *Blood* 2012; 120:5185-7; PMID:23024237; <http://dx.doi.org/10.1182/blood-2012-07-441030>
- Sebastian M, Kiewe P, Schuette W, Brust D, Peschel C, Schneller F, Rühle KH, Nilius G, Ewert R, Lodziewski S, et al. Treatment of malignant pleural effusion with the trifunctional antibody catumaxomab (Removab) (anti-EpCAM x Anti-CD3): results of a phase 1/2 study. *J Immunother* 2009; 32:195-202; PMID:19238019; <http://dx.doi.org/10.1097/CJI.0b013e318195b5bb>
- Sebastian M, Kuemmel A, Schmidt M, Schmittel A. Catumaxomab: a bispecific trifunctional antibody. *Drugs Today (Barc)* 2009; 45:589-97; PMID:19927225; <http://dx.doi.org/10.1358/dot.2009.45.8.1401103>
- Sebastian M, Passlick B, Friccius-Quecke H, Jäger M, Lindhofer H, Kanniss F, Wiewrodt R, Thiel E, Buhl R, Schmittel A. Treatment of non-small cell lung cancer patients with the trifunctional monoclonal antibody catumaxomab (anti-EpCAM x anti-CD3): a phase I study. *Cancer Immunol Immunother* 2007; 56:1637-44; PMID:17410361; <http://dx.doi.org/10.1007/s00262-007-0310-7>
- Röthlisberger D, Honegger A, Plückthun A. Domain interactions in the Fab fragment: a comparative evaluation of the single-chain Fv and Fab format engineered with variable domains of different stability. *J Mol Biol* 2005; 347:773-89; PMID:15769469; <http://dx.doi.org/10.1016/j.jmb.2005.01.053>

10. Mabry R, Gilbertson DG, Frank A, Vu T, Ardourel D, Ostrand C, Stevens B, Julien S, Franke S, Meengs B, et al. A dual-targeting PDGFRbeta/VEGF-A molecule assembled from stable antibody fragments demonstrates anti-angiogenic activity in vitro and in vivo. *MAbs* 2010; 2:20-34; PMID:20065654; <http://dx.doi.org/10.4161/mabs.2.1.10498>
11. Mabry R, Lewis KE, Moore M, McKernan PA, Bukowski TR, Bontadelli K, Brender T, Okada S, Lum K, West J, et al. Engineering of stable bispecific antibodies targeting IL-17A and IL-23. *Protein Eng Des Sel* 2010; 23:115-27; PMID:20022918; <http://dx.doi.org/10.1093/protein/gzp073>
12. Orcutt KD, Ackerman ME, Cieslewicz M, Quiroz E, Slusarczyk AL, Frangioni JV, Witttrup KD. A modular IgG-scFv bispecific antibody topology. *Protein Eng Des Sel* 2010; 23:221-8; PMID:20019028; <http://dx.doi.org/10.1093/protein/gzp077>
13. Michaelson JS, Demarest SJ, Miller B, Amatucci A, Snyder WB, Wu X, Huang F, Phan S, Gao S, Doern A, et al. Anti-tumor activity of stability-engineered IgG-like bispecific antibodies targeting TRAIL-R2 and LTbetaR. *MAbs* 2009; 1:128-41; PMID:20061822; <http://dx.doi.org/10.4161/mabs.1.2.7631>
14. Jordan JL, Arndt JW, Hanf K, Li G, Hall J, Demarest S, Huang F, Wu X, Miller B, Glaser S, et al. Structural understanding of stabilization patterns in engineered bispecific Ig-like antibody molecules. *Proteins* 2009; 77:832-41; PMID:19626705; <http://dx.doi.org/10.1002/prot.22502>
15. Andris-Widhopf J, Rader C, Steinberger P, Fuller R, Barbas CF 3rd. Methods for the generation of chicken monoclonal antibody fragments by phage display. *J Immunol Methods* 2000; 242:159-81; PMID:10986398; [http://dx.doi.org/10.1016/S0022-1759\(00\)00221-0](http://dx.doi.org/10.1016/S0022-1759(00)00221-0)
16. Nissim A, Hoogenboom HR, Tomlinson IM, Flynn G, Midgley C, Lane D, Winter G. Antibody fragments from a 'single pot' phage display library as immunochemical reagents. *EMBO J* 1994; 13:692-8; PMID:7508862
17. Mahon CM, Lambert MA, Glanville J, Wade JM, Fennell BJ, Krebs MR, Armellino D, Yang S, Liu X, O'Sullivan CM, et al. Comprehensive interrogation of a minimalist synthetic CDR-H3 library and its ability to generate antibodies with therapeutic potential. *J Mol Biol* 2013; 425:1712-30; PMID:23429058; <http://dx.doi.org/10.1016/j.jmb.2013.02.015>
18. Bazin-Redureau MI, Renard CB, Scherrmann JM. Pharmacokinetics of heterologous and homologous immunoglobulin G, F(ab')₂ and Fab after intravenous administration in the rat. *J Pharm Pharmacol* 1997; 49:277-81; PMID:9231345; <http://dx.doi.org/10.1111/j.2042-7158.1997.tb06795.x>
19. Barbas CF 3rd, Bain JD, Hoekstra DM, Lerner RA. Semisynthetic combinatorial antibody libraries: a chemical solution to the diversity problem. *Proc Natl Acad Sci U S A* 1992; 89:4457-61; PMID:1584777; <http://dx.doi.org/10.1073/pnas.89.10.4457>
20. Bostrom J, Lee CV, Haber L, Fuh G. Improving antibody binding affinity and specificity for therapeutic development. [xiii]. *Methods Mol Biol* 2009; 525:353-76, xiii; PMID:19252851; http://dx.doi.org/10.1007/978-1-59745-554-1_19
21. King AC, Woods M, Liu W, Lu Z, Gill D, Krebs MR. High-throughput measurement, correlation analysis, and machine-learning predictions for pH and thermal stabilities of Pfizer-generated antibodies. *Protein Sci* 2011; 20:1546-57; PMID:21710487; <http://dx.doi.org/10.1002/pro.680>
22. Chaudhary VK, Gallo MG, FitzGerald DJ, Pastan I. A recombinant single-chain immunotoxin composed of anti-Tac variable regions and a truncated diphtheria toxin. *Proc Natl Acad Sci U S A* 1990; 87:9491-4; PMID:2251289; <http://dx.doi.org/10.1073/pnas.87.23.9491>
23. Zahnd C, Sarkar CA, Plückthun A. Computational analysis of off-rate selection experiments to optimize affinity maturation by directed evolution. *Protein Eng Des Sel* 2010; 23:175-84; PMID:20130104; <http://dx.doi.org/10.1093/protein/gzp087>
24. He F, Becker GW, Litowski JR, Narhi LO, Brems DN, Razinkov VI. High-throughput dynamic light scattering method for measuring viscosity of concentrated protein solutions. *Anal Biochem* 2010; 399:141-3; PMID:19995543; <http://dx.doi.org/10.1016/j.ab.2009.12.003>
25. Finlay WJ, Cunningham O, Lambert MA, Darmanin-Sheehan A, Liu X, Fennell BJ, Mahon CM, Cummins E, Wade JM, O'Sullivan CM, et al. Affinity maturation of a humanized rat antibody for anti-RAGE therapy: comprehensive mutagenesis reveals a high level of mutational plasticity both inside and outside the complementarity-determining regions. *J Mol Biol* 2009; 388:541-58; PMID:19285987; <http://dx.doi.org/10.1016/j.jmb.2009.03.019>
26. Finlay WJ, Bloom L, Cunningham O. Optimized generation of high-affinity, high-specificity single-chain Fv antibodies from multiantigen immunized chickens. *Methods Mol Biol* 2011; 681:383-401; PMID:20978977; http://dx.doi.org/10.1007/978-1-60761-913-0_21
27. Jespers L, Schon O, Famm K, Winter G. Aggregation-resistant domain antibodies selected on phage by heat denaturation. *Nat Biotechnol* 2004; 22:1161-5; PMID:15300256; <http://dx.doi.org/10.1038/nbt1000>
28. Cummins E, Luxenberg DP, McAleese F, Widom A, Fennell BJ, Darmanin-Sheehan A, Whitters MJ, Bloom L, Gill D, Cunningham O. A simple high-throughput purification method for hit identification in protein screening. *J Immunol Methods* 2008; 339:38-46; PMID:18760282; <http://dx.doi.org/10.1016/j.jim.2008.07.016>
29. Myszka DG. Improving biosensor analysis. *J Mol Recognit* 1999; 12:279-84; PMID:10556875; [http://dx.doi.org/10.1002/\(SICI\)1099-1352\(199909/10\)12:5<279::AID-JMR473>3.0.CO;2-3](http://dx.doi.org/10.1002/(SICI)1099-1352(199909/10)12:5<279::AID-JMR473>3.0.CO;2-3)
30. Kortt AA, Gruen LC, Oddie GW. Influence of mass transfer and surface ligand heterogeneity on quantitative BIAcore binding data. Analysis of the interaction of NC10 Fab with an anti-idiotypic Fab'. *J Mol Recognit* 1997; 10:148-58; PMID:9408831; [http://dx.doi.org/10.1002/\(SICI\)1099-1352\(199705/06\)10:3<148::AID-JMR360>3.0.CO;2-F](http://dx.doi.org/10.1002/(SICI)1099-1352(199705/06)10:3<148::AID-JMR360>3.0.CO;2-F)